

## Patterns of Human Local Cerebral Glucose Metabolism During Epileptic Seizures

**Abstract.** Ictal patterns of local cerebral metabolic rate have been studied in epileptic patients by positron computed tomography with  $^{18}\text{F}$ -labeled 2-fluoro-2-deoxy-D-glucose. Partial seizures were associated with activation of anatomic structures unique to each patient studied. Ictal increases and decreases in local cerebral metabolism were observed. Scans performed during generalized convulsions induced by electroshock demonstrated a diffuse ictal increase and postictal decrease in cerebral metabolism. Petit mal absences were associated with a diffuse increase in cerebral metabolic rate. The ictal fluorodeoxyglucose patterns obtained from patients do not resemble autoradiographic patterns obtained from common experimental animal models of epilepsy.

Anatomic structures activated during experimentally induced epileptic seizures in animals have been revealed (1) by the 2- $^{14}\text{C}$ deoxy-D-glucose (2DG) autoradiography technique of Sokoloff *et al.* (2). Although this technique was designed for steady-state conditions, and although absolute local cerebral metabolic rate for glucose cannot yet be calculated for transient events such as seizures, nevertheless, visual inspection and semiquantitative analysis of patterns of ictal activation can yield meaningful information concerning the anatomic substrates of seizure-related behavior. Analogous images of local cerebral glucose metabolism in patients have now

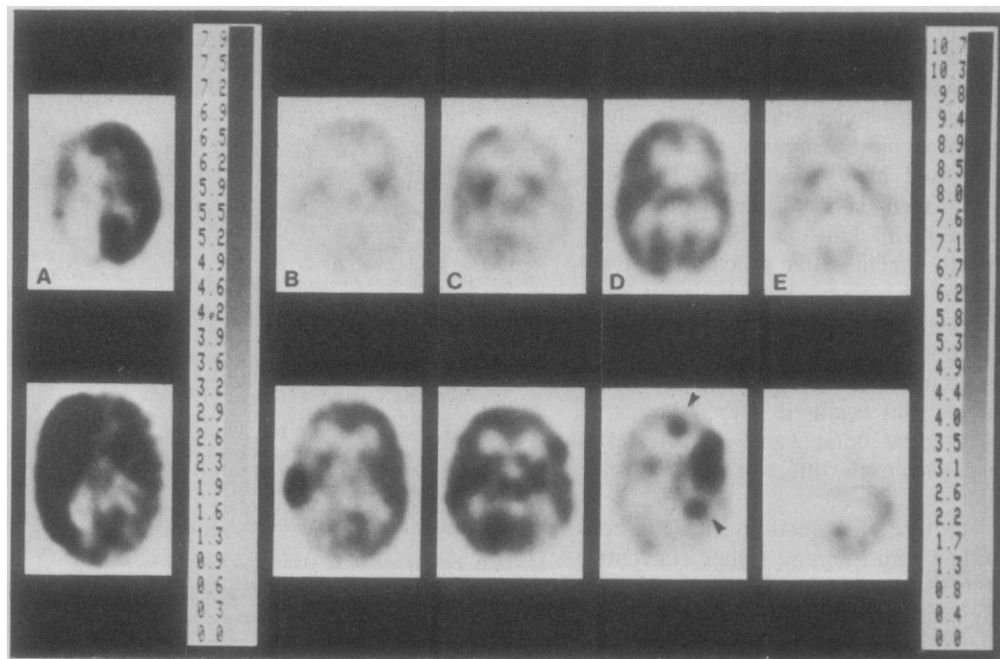
been obtained for a variety of epileptic seizure types using positron computed tomography (PCT) (3) with  $^{18}\text{F}$ -labeled 2-fluoro-2-deoxy-D-glucose (FDG) (4). These studies reveal patterns of functional cerebral activation during various clinical ictal states and allow comparison with those obtained by 2DG autoradiography during experimental seizures in animal models of epilepsy.

Quantitative ictal and interictal (or control) FDG studies were carried out during partial seizures, petit mal absences, and electroshock-induced generalized tonic clonic convulsions. Scanning with the tomograph (ECAT) (5, 6) was begun 40 minutes after intravenous

injection of 10 mCi of FDG labeled with  $^{18}\text{F}$  (7). Calculated values of ictal glucose consumption (8) actually represent a weighted average of ictal, postictal, and interictal metabolism and have no absolute quantitative significance. Although these values will not be specifically discussed in this report, they are indicated for each patient in the figures. The electroencephalogram (EEG) and behavior were monitored before, during, and for at least 1/2 hour after FDG injection. For ten patients, gold disk electrodes were applied according to the International 10-20 System, while one patient was monitored from bipolar stainless steel depth electrodes [stereotaxically implanted into hippocampus, hippocampal gyrus, and amygdala (9)], stainless steel skull nails, and stainless steel sphenoidal electrodes as part of a routine evaluation for surgical therapy of medically intractable partial seizures (10).

Partial seizures were studied in one patient with epilepsy partialis continua and in four patients with seizures that recurred spontaneously from three to nine times during the first 30 minutes after FDG injection. Two separate ictal studies were carried out on different days for one of these latter patients. Repeat scans were also obtained for each

Fig. 1. Representative planes of section of interictal (top row) and ictal (bottom row) FDG scans from five patients with partial seizures. Scales in this and the following figures indicate the calculated local cerebral metabolic rate for glucose in milligrams per 100 g per minute. Scans B to E are all displayed to the same scale, chosen to best illustrate values for maximal ictal activation. Scan A is scaled differently as a result of technical difficulties in displaying data. The number of ictal events occurring in the first 1/2 hour after FDG injection are indicated for each patient below. X-ray tomography scans were abnormal for patient A, who had left-hemisphere atrophy, and patient E, who had a small right-occipital glioma. (A) Ictal activation of the entire left hemisphere occurred with nine seizures that originated electrically in the left parietal area and spread to involve both sides of the body, the right side more than the left. (B) Selective ictal activation of the left perisylvian area occurred within a larger zone of interictal hypometabolism during seven seizures that were confined electrographically to left temporal and central electrodes and behaviorally to the right arm and face. A second ictal scan in this patient demonstrated the same pattern. (C) Hypermetabolism of the entire brain—prominent in the right precentral area, which was hypometabolic interictally—accompanied epilepsy partialis continua involving the left leg and arm. The ictal EEG contained no localizing abnormalities. (D) Seven partial complex seizures with twitching of the left side of the mouth and head and eye turning to the left were associated with increased metabolic activity in right temporal and frontal structures, including discrete activation of hippocampus and cingulate cortex (arrows) and decreased metabolic activity elsewhere. (E) Three seizures that originated in the right occiput and spread into the right temporal lobe began with formed visual auras in the left visual field progressing to partial complex symptomatology. This was associated with hypermetabolism of the right occipital and temporal lobes and hypometabolism elsewhere.



patient at a time when no spontaneous seizures occurred between FDG injection and PCT measurements. As noted previously (11), interictal FDG scans contained hypometabolic zones that included the epileptic focus determined by EEG. Ictal scans revealed focal, multifocal, hemispheric, and generalized increases in estimated metabolic rate ranging from two to six times the measured interictal values for homotopic regions (Fig. 1). The areas of ictal hypermetabolism did not always correspond to the zones of hypometabolism observed interictally; they included, but were not necessarily confined to, the site of EEG-recorded ictal onset and spread. Although these patterns differed from patient to patient, the two ictal FDG scans obtained from the same patient on different days demonstrated essentially identical patterns. Three patients also showed a general increase in cerebral metabolic activity beyond the focal zones of hypermetabolism (Fig. 1, A to C). For the other two, the remainder of the brain demonstrated a relative hypometabolism compared to interictal measurements (Fig. 1, D and E).

The patient with stereotaxically implanted depth electrodes was studied during a single 72-second complex partial seizure induced by electrical stimulation of the right hippocampus (12, 13) immediately after FDG injection. The scan revealed right temporal lobe hypometabolism compared with the control interictal scan, which was also made while depth electrodes were in place (Fig. 2).

Because of the temporal limitation of

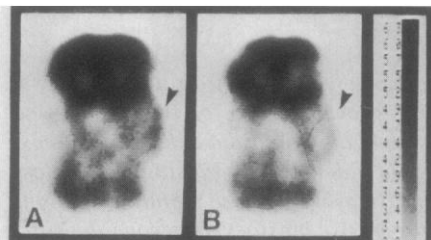
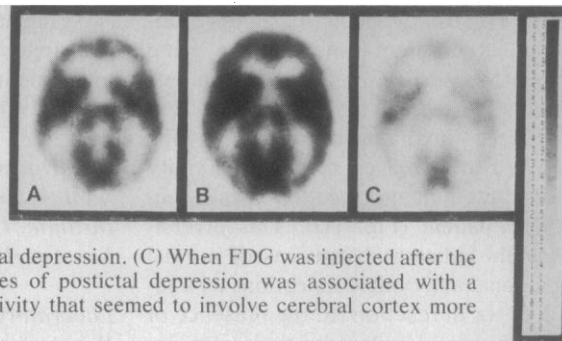


Fig. 2. Representative planes of interictal (A) and ictal (B) scans from patient with electrical stimulation of right hippocampus. (A) The interictal FDG scan demonstrated hypometabolism of the left temporal lobe, which was also determined to be the site of the epileptogenic lesion. The right temporal lobe looked metabolically normal (arrow). (B) Electrical stimulation of the right hippocampus immediately after FDG injection resulted in 72 seconds of electrical afterdischarge associated with a brief lapse of consciousness, and reduction in metabolic activity in the right temporal lobe (arrow) excluding the hippocampus.

Fig. 3. Representative sections from control (A), ictal (B), and postictal (C) FDG scans of a patient during serial electroconvulsive shock treatments. In (B), metabolic activity increased compared with the control (A) as a result of a generalized tonic clonic convulsion lasting 20 seconds and followed by 7.5 minutes of postictal depression. (C) When FDG was injected after the seizure was completed, 9 minutes of postictal depression was associated with a diffuse decrease in metabolic activity that seemed to involve cerebral cortex more than basal ganglia.



the FDG method, it is impossible to determine the exact relationship between these observed metabolic alterations and the specific ictal, postictal, and interictal electrical and behavioral events that occurred during the 40 minutes between FDG injection and PCT scanning. Consequently, the relative hypometabolism observed near the site of electrical stimulation in one patient and in the rest of the brain in two others with spontaneous seizures could represent metabolic correlates of ictal or postictal neuronal activity. The effect of postictal depression on patterns of local cerebral glucose metabolism were determined from ictal, postictal, and control studies on a patient who underwent a series of electroconvulsive shock treatments. At the time of bilateral electroshock, FDG was injected to obtain an ictal scan. In a second study carried out several days later, FDG was injected on termination of the clonic phase and onset of EEG depression to obtain a postictal scan. A third control scan was obtained between electroconvulsive treatments. The ictal scan revealed an increase in global cerebral metabolic rate compared with the control (Fig. 3, A and B), whereas the postictal scan revealed a decrease in global cerebral metabolic rate (Fig. 3, A and C). The pattern of postictal hypometabolism appeared to be more profound for cortical than for deep gray-matter structures.

Four untreated patients with petit mal epilepsy were studied by injecting FDG just before 10 minutes of hyperventilation. The frequency of induced absences during this time ranged from one to four per minute. Control studies were carried out several months later after successful drug therapy. Ten minutes of hyperventilation failed to induce any absences in three patients and only infrequent absences in the fourth. No abnormalities in the FDG scan were noted when hyperventilation was not associated with absences. When hyperventilation produced absences, accompanied by classical gen-

eralized three per second spike and wave EEG discharges, global cerebral metabolic rate for glucose was increased 2 to 3.5 times over the control; the patterns of distribution of glucose metabolism observed on ictal and control FDG scans did not seem to differ, however (Fig. 4). The degree of hypermetabolism was not correlated with the frequency or duration of petit mal absences.

Previous 2DG autoradiographic investigations of experimental epilepsy have demonstrated anatomic patterns of ictal metabolism that vary with the animal species, the type of epileptogenic agent, and the site of ictal onset, but appear to be stereotyped within these subgroups (1). Areas of ictal activation have been interpreted to indicate the major pathways of propagation of ictal discharge and, in general, have agreed well with known anatomic connections of the epileptic focus. In contrast, FDG patterns obtained from six patients during partial seizures have been unique to each patient studied, despite the fact that the ictal discharge seemed to originate in the temporal lobe in three and spread to the temporal lobe in at least two others.

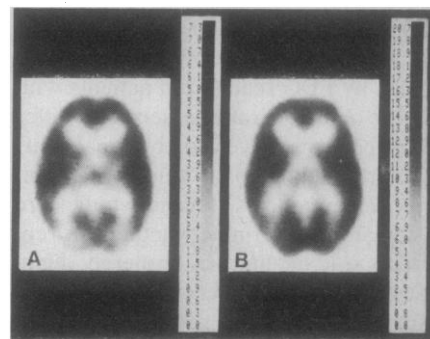


Fig. 4. Representative sections from control (A) and ictal (B) FDG scans of a patient with petit mal. (A) A normal FDG scan was obtained during 10 minutes of hyperventilation following successful treatment with valproic acid. (B) Prior to treatment, 10 minutes of hyperventilation resulted in 11 absences totaling 3.5 minutes, associated with a diffuse increase in metabolic activity. Ictal and control patterns are identical.

Since two similar ictal scans were obtained at different times on the same patient, these FDG patterns may be reproducible for each patient. Epileptiform discharges involving the temporal lobe resulted in increased metabolic activity in discrete limbic projection sites in only one patient (Fig. 1D). This diversity could indicate aberrations of normal functional anatomic connections as a result of, or in reaction to, the presence of a chronic focal epileptogenic lesion.

The FDG scan obtained after electroconvulsive shock therapy demonstrated that postictal depression is associated with a relative decrease in glucose metabolism. Consequently, the areas of relative hypometabolism seen on some ictal FDG scans during partial seizures may represent metabolic correlates of postictal phenomena. Ictal hypometabolism might also reflect surround inhibition (14). Although active inhibitory synaptic events appear to require energy (15), hypometabolism could occur at the efferent projection sites of inhibited neurons.

Two putative experimental models for clinical petit mal have been studied with 2DG autoradiography. Intracerebroventricular opioid peptides specifically activate limbic structures (16), whereas intramuscular penicillin fails to alter cerebral metabolism (Wada and Kobayashi, personal communication). The FDG scans of patients with petit mal revealed a reproducible diffuse increase in metabolic activity, suggesting that the pathological mechanisms for clinical and experimental petit mal are not the same. Although FDG scans failed to identify specific anatomic activation during petit mal seizures, a deep discrete generator responsible for initiation of the more generalized discharges could still be missed by this technique.

Patterns of ictal metabolic activity revealed by FDG scans from patients with partial and generalized seizures differ from patterns revealed by analogous 2DG autoradiographic studies of common animal models. Further studies are necessary to determine whether this represents true qualitative, or merely quantitative, differences between clinical and experimental epilepsy. It is necessary to bridge this gap between animal and human research in order to test hypotheses and develop clinically useful applications. Positron computed tomography, coupled with surface and depth electrode EEG recordings (10, 11), may provide a greater opportunity to determine which of the extensive electrophysiologic, metabolic, and anatomic data obtained from

experimental models are relevant to human epileptic conditions and, ultimately, to pursue investigations into basic mechanisms of human epilepsy directly.

JEROME ENGEL, JR.

Departments of Neurology and Anatomy and Brain Research Institute, UCLA School of Medicine, Los Angeles, California 90024

DAVID E. KUHL

Laboratory of Nuclear Medicine and Department of Radiological Sciences, UCLA School of Medicine

MICHAEL E. PHELPS

Division of Biophysics, Laboratory of Nuclear Medicine, and Department of Radiological Sciences, UCLA School of Medicine

#### References and Notes

1. Y. Ben-Ari, D. Riche, E. Tremblay, G. Charton, *C.R. Acad. Sci. Ser. D* **290**, 1149 (1980); Y. Ben-Ari, E. Tremblay, D. Riche, G. Ghilini, R. Naquet, *Neuroscience* **6**, 1361 (1981); R. C. Collins, *Brain Res.* **150**, 487 (1978); *ibid.*, p. 503; and T. V. Caston, *Neurology* **29**, 705 (1979); R. C. Collins, C. Kennedy, L. Sokoloff, F. Plum, *Arch. Neurol.* **33**, 536 (1976); R. C. Collins, M. McLean, J. Olney, *Life Sci.* **27**, 855 (1980); J. Engel, Jr., L. Wolfson, L. Brown, *Ann. Neurol.* **3**, 538 (1978); W. F. Caveness, M. Kato, B. L. Malamut, S. Hosokawa, S. Wakisaka, R. R. O'Neill, *ibid.* **7**, 213 (1980); S. Hosokawa, T. Iguchi, W. F. Caveness, M. Kato, R. R. O'Neill, S. Wakisaka, B. L. Malamut, *ibid.*, p. 222; M. Kato, B. L. Malamut, W. F. Caveness, S. Hosokawa, S. Wakisaka, R. R. O'Neill, *ibid.*, p. 204; M. Klit and C. E. Poletti, *Science* **204**, 641 (1979); R. E. Watson and A. Siegel, in *The Amygdaloid Complex*, Y. Ben-Ari, Ed. (Elsevier/North-Holland, Amsterdam, 1979), p. 453.
2. L. Sokoloff *et al.*, *J. Neurochem.* **28**, 897 (1977).
3. M. E. Phelps, E. J. Hoffman, N. A. Mullani, M. M. Ter-Pogossian, *J. Nucl. Med.* **16**, 210 (1975).
4. M. E. Phelps, S. C. Huang, E. J. Hoffman, C. E. Selin, D. E. Kuhl, *Ann. Neurol.* **6**, 371 (1979); M. Reivich *et al.*, *Circ. Res.* **44**, 127 (1979).
5. M. E. Phelps, E. J. Hoffman, S. C. Huang, D. E. Kuhl, *J. Nucl. Med.* **19**, 635 (1978).
6. The spatial resolution used in these studies was 1.6 by 1.6 cm in the tomographic plane and  $1.6 \pm 0.2$  cm in the axial direction measured at full width, half maximum of a line source.
7. H. R. Barrio, N. S. McDonald, G. D. Robinson, Jr., A. Najafi, J. S. Cook, D. E. Kuhl, *J. Nucl. Med.* **22**, 372 (1981).
8. S. C. Huang, M. E. Phelps, E. J. Hoffman, K. Sideris, C. J. Selin, D. E. Kuhl, *Am. J. Physiol.* **238**, E69 (1980); S. C. Huang, M. E. Phelps, E. J. Hoffman, D. E. Kuhl, *J. Cereb. Blood Flow Metab.* **1**, 391 (1981).
9. P. H. Crandall, R. D. Walter, R. W. Rand, *J. Neurosurg.* **20**, 827 (1963).
10. J. Engel, Jr., P. H. Crandall, R. Rausch, in *The Clinical Neurosciences*, R. N. Rosenberg, R. G. Grossman, S. Schochet, E. R. Heinz, W. Willis, Eds. (Churchill Livingstone, New York, in press); J. Engel, Jr., R. Rausch, J. P. Lieb, P. H. Crandall, *Ann. Neurol.* **9**, 215 (1981).
11. J. Engel, Jr., D. E. Kuhl, M. E. Phelps, in *Status Epilepticus: Mechanisms of Brain Damage and Treatment*, A. V. Delgado Escueta, C. G. Wasterlain, D. M. Treiman, R. J. Porter, Eds. (Raven, New York, in press); *Trans. Am. Neurol. Assoc.* **105**, 74 (1981); in *Advances in Epileptology*, H. Akimoto, H. Kazamatsuri, M. Seino, Eds. (Raven, New York, in press); and J. C. Mazziotta, *Ann. Neurol.*, in press; J. Engel, Jr., W. J. Brown, D. E. Kuhl, M. E. Phelps, J. C. Mazziotta, P. H. Crandall, *ibid.*; J. Engel, Jr., D. E. Kuhl, M. E. Phelps, P. H. Crandall, *ibid.*; D. E. Kuhl, J. Engel, Jr., M. E. Phelps, C. Selin, *ibid.* **8**, 348 (1980).
12. D. G. Cherlow, A. M. Dymond, P. H. Crandall, R. D. Walter, E. A. Serafetinides, *Arch. Neurol.* **34**, 527 (1977).
13. Electrical stimulation of one bipolar hippocampal electrode was carried out with a 12-second train of 0.1-msec biphasic 4-mA square-wave pulses at 60 Hz.
14. D. A. Prince and B. J. Wilder, *Arch. Neurol.* **16**, 194 (1967).
15. R. F. Ackermann, D. M. Finch, T. L. Babb, J. Engel, Jr., *Soc. Neurosci. Abstr.* **7**, 457 (1981).
16. S. J. Henrikson, F. E. Bloom, N. Ling, R. Guillemain, *ibid.* **3**, 293 (1977); H. T. Chugani, R. F. Ackermann, D. C. Chugani, J. Engel, Jr., *Ann. Neurol.* **12**, 93 (1982).
17. Supported by DOE contract DE-AM03-76-SF00012 and by grants GM-24839, NS-15654, and NS-02808 from the Public Health Service.

15 March 1982; revised 1 June 1982

## Development of Mouse Embryos in vitro: Preimplantation to the Limb Bud Stage

**Abstract.** *Mouse embryos were grown successfully in vitro from the blastocyst stage to the limb bud stage. Mouse blastocysts grown in vitro for 10 days showed blood circulation in the yolk sac, forelimb buds, and the primordia of liver, pancreas, and lungs. These characteristics are indicative of a developmental stage equivalent to one-half of the total gestation period in utero. Improvements in culture conditions from days 7 to 9 have made it feasible to culture mouse blastocysts beyond the early somite stage.*

In the 1960's and early 1970's, investigators found means of culturing fertilized mouse ova in simple media up to the blastocyst stage (1). However, it has been difficult to grow mouse blastocysts in vitro beyond the egg-cylinder stage. Many investigators have cultured mouse embryos from the blastocyst stage to the egg-cylinder stage (2); few such blastocysts have reached the early somite stages (3) and none have survived beyond these stages. At the early somite

stage, the blood circulation in the yolk sac is not established and the anterior neuropore is open. The limb buds and the primordia of the lung, liver, and pancreas are not yet present (3). We report here the successful culture of mouse embryos from the blastocyst stage to the limb bud stage.

Blastocysts (3.5 days of gestation) were obtained from random-bred CF1 mice (4) and cultured as described in Table 1. Of 86 blastocysts cultured for 10